CHAPTER 7

CLERODENDRUM INFORTUNATUM EXTRACT: NATURAL CORROSION INHIBITOR FOR MILD STEEL IN ACID MEDIA

The anti-corrosion properties of leaves and roots extracts of *Clerodendrum infortunatum* (CILE and CIRE) on mild steel are discussed here. The comparison of inhibition efficiency in two different acids, i.e., 1 M HCl and 0.5 M H_2SO_4, also have been studied. *Clerodendrum infortunatum* belongs to Lamiaceae family. Physicochemical, electrochemical, surface morphological and quantum mechanical studies have been employed as corrosion monitoring techniques. *Clerodendrum infortunatum* is comprised of diverse phytochemical constituents responsible for their pharmacological activities. Ethanolic extracts of CILE and CIRE contains saponins, flavonoids, steroids, tannins, and reducing sugars. Terpenoids are mainly present in the roots and negligibly present in the leaves, while alkaloids are absent in both extracts[185]. Clerodin and scutellarin are major diterpenoid and flavonoid, respectively, found in *Clerodendrum infortunatum* plants[186],[187]. Their structures are shown in Fig. 7.1. The inhibitive performance of CILE and CIRE is assessed with the concept that adsorption of its phytochemicals onto the mild steel surface made a protective barrier to the metal surface. Clerodin and scutellarin are subjected to theoretical calculations as major terpenoid and flavonoid, respectively, present in *Clerodendrum infortunatum* extracts.

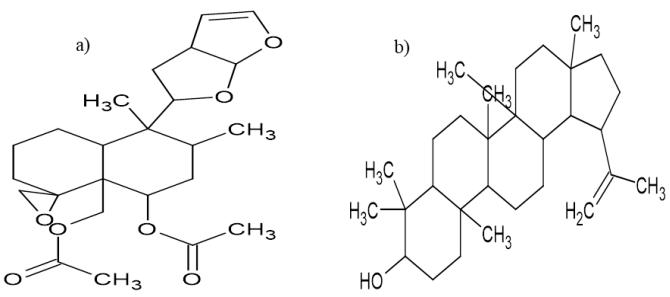

Fig. 7.1: Structure of a) clerodin b) scutellarin

Clerodendrum infortunatum

Results and discussions

Phytochemical screening of CILE and CIRE

Standard phytochemical screening tests were carried out to identify the phytochemicals in CILE and CIRE qualitatively, and the results are given in Table 7.1.

Table 7.1: Phytochemical screening of CILE and CIRE

Sl. No.	Compounds	Tests	Results of CILE	Results of CIRE
1	Alkaloids	Mayer's reagent	−−	−−
2	Steroids	Salkowaski's test	++	++
3	Phenolic compounds	Potassium ferrocyanide test	++	++
4	Flavanoids	Sodium hydroxide test	++	++
5	Saponins	Froth test	++	++
6	Tannins	Lead acetate test	++	++
7	Cardiac glycosides	Conc. sulphuric acid test	−−	−−
8	Coumarin	Alcoholic NaOH test	++	++
9	Terpenoids	Conc. sulphuric acid test	−−	++

++ (present), − − (Absent)

The phytochemical screening data were found to agree with the literature survey.

FTIR spectroscopy

Phytochemicals of plant extracts have functional groups with heteroatoms such as N, O etc., which are considered adsorption centres. It can be established by FTIR analysis of ethanolic CILE and CIRE. Fig. 7.2 a) and Fig. 7.2 b) show FTIR spectra of ethanolic CILE and CIRE, respectively. The broad absorption band at 3281 cm^{-1} for CILE and 3267 cm^{-1} for CIRE can be assigned to O–H stretching vibration. Peak corresponds to C–H stretching vibration observed at 2918 cm^{-1} for CILE and 2921 cm^{-1} for CIRE. The weak band at 2113 cm^{-1} for CILE and at 2111 cm^{-1} for CIRE may be ascribed to C-O stretching vibrations. Aliphatic and aromatic C=C stretching vibration appears at 1631 cm^{-1} for CILE and at 1603 cm^{-1} for CIRE. C-O-H in-plane bending vibrations seems at 1401 and 1413 cm^{-1} for CILE and CIRE, respectively. It may be due to the presence of phenolic acids in the extracts. The absorption bands below 1,000 cm^{-1}

can be attributed to the C–H bending vibrations. FTIR results showed that the ethanolic extracts of both CILE and CIRE consisted of functional groups like O–H, C–O, C=C, and aromatic rings, which can form an adsorption layer on the metal surface by donating pi-electrons.

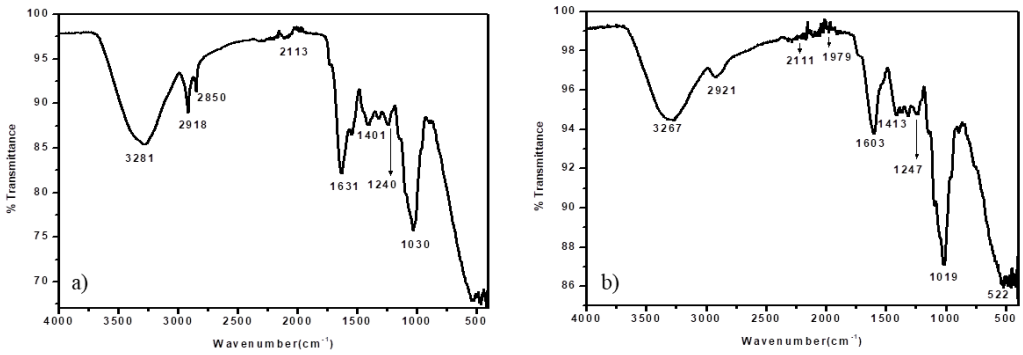

Fig. 7.2: FTIR spectra of a) CILE b) CIRE

Weight loss measurements

❖ ***Effect of concentration***

Table 7.2 represents the variation of corrosion rate (υ) and inhibition efficiency (η%) for mild steel in 1 M HCl and 0.5 M H_2SO_4 without and with CILE and CIRE at room temperatures. It has been observed from Table 7.2 that the corrosion rate of mild steel was diminished by introducing both leaves and roots extract of *Clerodendrum infortunatum* into acid media, indicating the corrosion mitigation power of the metal immersed in the presence of the extracts. Inspection of Table 7.2 also realized that inhibition efficiency is directly proportional to the concentration of extracts. The anti-corrosion performance of CILE and CIRE was ascribed to the adsorption of the phytochemical constituents of the extract at the mild steel-acid solution interface. Thus, it hindered active corrosion sites on the mild steel and decreased the rate of corrosion[188]. It was pointed out that the extract of the roots exhibits superior performance than leaves extract as a corrosion inhibitor for mild steel in both acid media. On comparing the

nature of acid media, HCl solution was more facilitated for corrosion inhibition than H_2SO_4 solution. Inhibition efficiency of 93.63% was obtained for roots and 87.56% for leaves at 303 K with 5 v/v% extract concentration in 1 M HCl. At the same time, in 0.5 M H_2SO_4, an inhibition efficiency of 65.73% was achieved for roots and 58.48% for leaves.

The variation in inhibition efficiency for roots and leaves was attributed to various phytochemicals present in CILE and CIRE. Notably, CIRE contains terpenoids, steroids, flavonoids, saponins, tannins and reducing sugars, while CILE contains all the phytochemicals in the roots except terpenoids. The presence of terpenoids in CIRE may be enhanced its anti-corrosion behaviour. The lone pair of electrons present in oxygen moieties of clerodin and scutellarin may be acted as an electron donor source.

The primary cause for the corrosion of mild steel in 1 M HCl is the adsorption of Cl^- ions onto the metal surface sites. The movement of inhibitor molecules is slower than Cl^- ions; therefore, Cl^- ions preferentially reach the metal surface. However, the inhibitor molecules can hinder Cl^- ions sterically and approach the metal surface sites[189]. The adsorption of halide ions in an inhibited solution on the metal surface is via oriented dipoles, which means cationic organic inhibitor molecules adsorb on the dipoles. So, it can be said that the rate of decrease in corrosion in the presence of both halide anions and inhibitor cations is a synergistic effect. This is why the greater inhibition efficiency of organic inhibitor molecules in HCl than H_2SO_4 medium. In the present investigation, the same is the observation, i.e., the anti-corrosion performance of CILE and CIRE were predominant in HCl solution compared to that in H_2SO_4 solution.

❖ ***Effect of temperature***

Fig. 7.3 shows the comparison of inhibition efficiency for mild steel in 1 M HCl and 0.5 M H_2SO_4 with various concentrations of CILE at different temperatures. Similar

plots for CIRE are exhibited in Fig. 7.4. It was noticed that the corrosion rate augmented with the rise in temperature with and without extracts. Inhibition efficiency was reduced with an increase in temperature in the presence of both extracts. It may be explained that the phytochemicals of both extracts were physically adsorbed on the mild steel surface.

Table 7.2: Weight loss measurements of mild steel with and without CILE and CIRE in 1 M HCl and 0.5 M H_2SO_4 at room temperature for 24 hrs

Inhibitor	Conc. (v/v %)	Corrosion rate (mm/yr)		Inhibition efficiency (η%)	
		1 M HCl	0.5 M H_2SO_4	1 M HCl	0.5 M H_2SO_4
CILE	Blank	3.95	35.57	-	-
	1	0.59	19.50	85.22	45.16
	2	0.50	17.98	87.34	49.45
	3	0.42	16.89	89.53	52.49
	4	0.30	15.55	92.48	56.28
	5	0.26	12.18	93.63	65.73
CIRE	1	1.83	20.90	53.42	41.24
	2	1.55	19.28	60.59	45.78
	3	0.88	18.21	77.58	48.79
	4	0.78	17.33	80.21	51.27
	5	0.49	14.76	87.56	58.48

Corrosion rates and inhibition efficiencies of CILE and CIRE from weight loss measurements in 1 M HCl and 0.5 M H_2SO_4 at 303, 313, 323 and 333 K are comparatively listed in Table 7.3. It has been observed from Table 7.3 that the inhibitive action of the extracts in different acid media was affected by temperature. In HCl and H_2SO_4 media, inhibition efficiency is reduced with the rise in temperature, which causes the decrease in stability of the adsorption layer[166]. This trend suggested that the phytochemicals of CILE and CIRE in HCl and H_2SO_4 media were physically adsorbed on the mild steel surface. It was also inferred from Table 7.3 that leaves and root extracts in the H_2SO_4 medium show a higher corrosion rate for mild steel at elevated temperatures. Inhibition efficiency decreased from 93.63% to 69.51% for 5 v/v% CIRE concentration, while the same concentration of CILE exhibited a sharp decrease from

87.56% to 68.23% in HCl solution when the temperature goes from 303 K to 333 K. Similarly, in the H_2SO_4 medium, corrosion inhibition capacity lowered from 65.73% to 43.67% for the highest CIRE concentration under-study, whereas, for CILE, efficacy reduced from 58.48% to 50.87% for the same concentration and temperature. An elevated temperature may be enhanced the desorption process of extracts from mild steel.

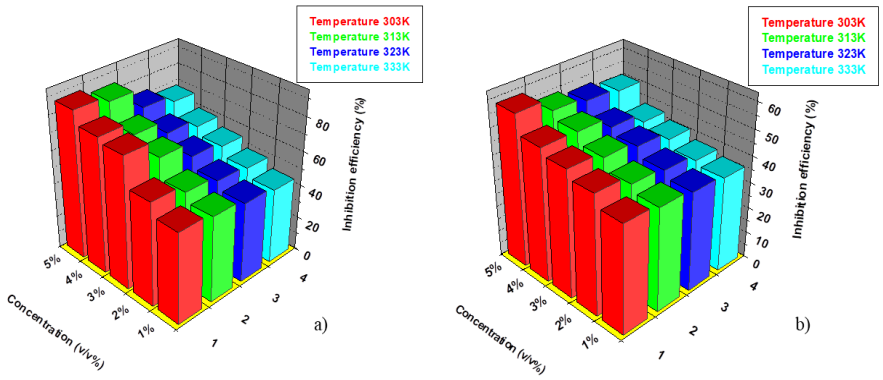

Fig. 7.3: Variation in inhibition efficiency of CILE in a) 1 M HCl b) 0.5 M H_2SO_4 at elevated temperatures

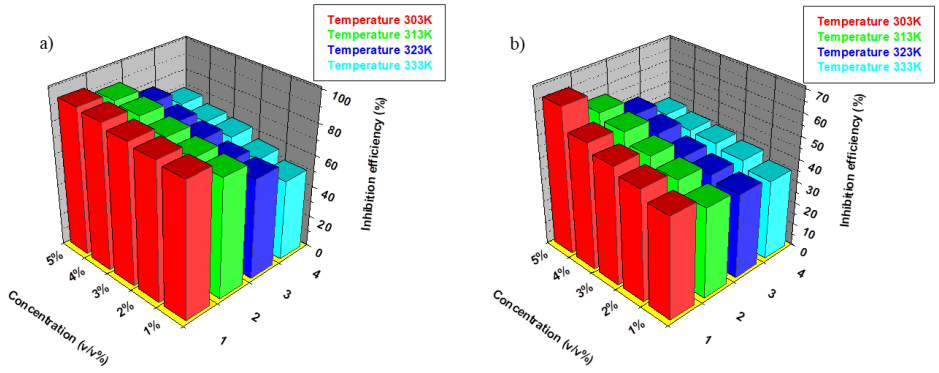

Fig. 7.4: Variation in inhibition efficiency of CIRE in a) 1 M HCl b) 0.5 M H_2SO_4 at elevated temperatures

Using the Arrhenius equation (41), the activation energy of metal corrosion was estimated. Fig. 7.5 a) and c) show the Arrhenius plots of log K vs 1/T for mild steel in 1 M HCl and 0.5 M H_2SO_4, respectively, with various CILE concentrations. Similar Arrhenius plots for CIRE are shown in Fig. 7.6 a) and Fig. 7.6 c). Thermodynamic parameters such as ΔH^* and ΔS^* values were rendered using equation (43) obtained from

transition state theory. From the slope and intercept of the plot of log K/T vs 1/T (Fig. 7.5 b) and Fig. 7.5 d)), ΔH^* and ΔS^* values for CILE inhibited metal corrosion were equated.

Table 7.3: Corrosion rate (υ) and inhibition efficiency (η%) of CIRE and CILE in 1 M HCl and 0.5 M H_2SO_4 at different temperatures for 24 hrs

Inhibitor/ Medium	Conc. (v/v%)	υ (303 K)	η% (303 K)	υ (313 K)	η% (313 K)	υ (323 K)	η% (323 K)	υ (333 K)	η% (333 K)
CILE/ 1 M HCl	Blank	3.95	-	13.11	-	22.05	-	31.77	-
	1	1.839	53.42	6.471	50.63	11.59	47.43	17.59	44.61
	2	1.556	60.59	5.822	55.59	10.63	51.77	16.01	49.60
	3	0.885	77.58	4.330	66.96	9.189	58.32	14.24	55.17
	4	0.781	80.21	3.602	72.52	7.807	64.59	12.63	60.21
	5	0.491	87.56	2.046	84.39	6.007	72.75	10.09	68.23
CILE/ 0.5 M H_2SO_4	Blank	35.57	-	58.27	-	86.25	-	106.2	-
	1	20.90	41.24	35.18	39.62	53.29	38.21	67.32	36.64
	2	19.28	45.78	33.65	42.25	51.12	40.73	65.70	38.17
	3	18.21	48.79	31.05	46.71	47.84	44.53	62.39	41.28
	4	17.33	51.27	28.56	50.98	45.82	46.87	60.23	43.31
	5	14.76	58.48	26.79	54.01	41.19	52.24	52.20	50.87
CIRE/ 1 M HCl	1	0.592	85.22	3.204	75.56	8.030	63.58	15.41	51.48
	2	0.508	87.34	2.865	78.14	7.664	65.24	13.68	56.94
	3	0.422	89.53	2.327	82.25	6.462	70.69	11.66	63.28
	4	0.306	92.48	1.672	87.24	5.849	73.47	11.01	65.32
	5	0.260	93.63	1.444	88.98	4.817	78.15	9.68	69.51
CIRE/ 0.5 M H_2SO_4	1	19.50	45.16	34.85	40.18	53.66	37.78	68.34	35.68
	2	17.98	49.45	31.78	45.46	51.63	40.13	64.66	39.14
	3	16.89	52.49	29.41	49.52	49.82	42.23	62.72	40.97
	4	15.55	56.28	26.65	54.26	45.73	46.97	61.89	41.75
	5	12.18	65.73	24.97	57.14	43.40	49.68	59.85	43.67

Similarly, ΔH^* and ΔS^* values for CIRE inhibited metal corrosion were calculated from Fig. 7.6 b) and d). Table 7.4 shows activation energy (E_a), pre-exponential factor (A), ΔH^* and ΔS^* values for mild steel corrosion with extracts of *Clerodendrum infortunatum* (CILE and CIRE) as inhibitors in acid media.

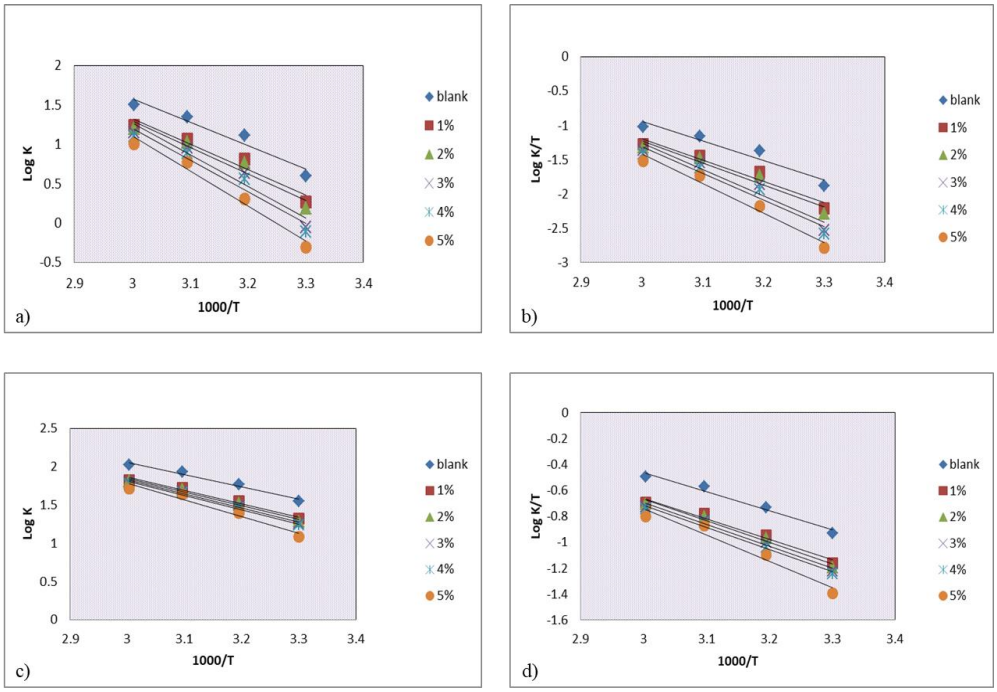

Fig. 7.5: a) Arrhenius plots b) log K/T vs 1000/T plots in 1 M HCl c) Arrhenius plots d) log K/T vs 1000/T in 0.5 M H_2SO_4 with and without CILE

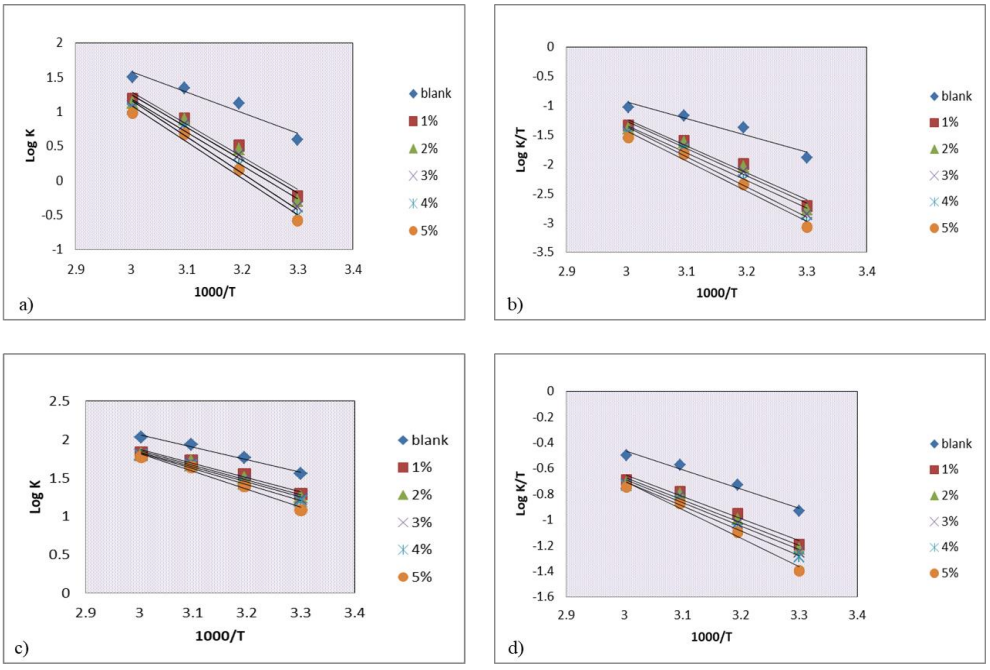

Fig. 7.6: a) Arrhenius plots b) log K/T vs 1000/T plots in 1 M HCl c) Arrhenius plots d) log K/T vs 1000/T in 0.5 M H_2SO_4 with and without CIRE

Table 7.4 revealed that the uninhibited acid media had lesser activation energy of mild steel corrosion than the inhibited acid media. The increase in E_a values with the concentration of CILE and CIRE lead to slow down the metal dissolution process. ΔH^*

and ΔS* values of the metal corrosion process were found to increase in the presence of CILE and CIRE. Positive values of the enthalpy of activation disclosed the endothermic character of metal corrosion. The observed ΔS* values for the blank experiment were negative, indicating that the rate-determining step in the metal dissolution process was an association rather than a dissociation step[190]. This association step represented a decrease in disorderliness in the formation of the activated complex from reactants. But, in the presence of CILE and CIRE as inhibitors in acids, disorderliness increased.

Adsorption isotherms

Adsorption characteristics of CILE and CIRE on mild steel surfaces were described by fitting the results obtained from weight loss measurements into various adsorption isotherm models. Langmuir adsorption isotherm was the best-fit isotherm for the adsorption of phytochemicals of both extracts by considering the tightness of the value R^2 to unity. The linear plots of Langmuir adsorption isotherm are shown in Fig. 7.7 for both extracts in 1 M HCl and 0.5 M H_2SO_4. Table 7.5 exhibits the adsorption parameters acquired from the Langmuir plots. On examining Table 7.5, it has come to the knowledge that K_{ads} value for CIRE in HCl solution was more prominent than all other inhibited solutions. This confirmed the strong adsorption of CIRE molecules onto the mild steel surface in the HCl medium[191]. The main reasons for the deviation of Langmuir isotherm slopes from unity are the interactions between adsorbed molecules on the mild steel and variations in the value of heat of adsorption.

The values of ΔG^0_{ads} are negative for both extracts. If its value is less negative than −20 kJ/mol, inhibitors adsorb physically on the metal surface but exceed −40 kJ/mol for the chemical adsorption of inhibitors. Herein, ΔG^0_{ads} values obtained for CILE and CIRE revealed mixed adsorption mode; physical and chemical adsorption in both acid media since ΔG^0_{ads} values were in between -20 kJ/mol and -40 kJ/mol.

Table 7.4: Thermodynamic parameters of mild steel corrosion with and without CILE/CIRE in 1 M HCl and 0.5 M H_2SO_4

Inhibitor/ Medium	Conc. (v/v %)	E_a (kJ mol^{-1})	A	ΔH^* (kJ mol^{-1})	ΔS^* (J $mol^{-1}K^{-1}$)
CILE/ 1 M HCl	Blank	57.24	3.58×10^{10}	54.60	-44.78
	1	62.13	1.15×10^{11}	59.49	-35.02
	2	64.16	2.22×10^{11}	61.52	-29.57
	3	76.79	1.91×10^{13}	74.15	7.84
	4	77.05	2.01×10^{13}	74.41	7.43
	5	85.53	3.25×10^{14}	82.89	31.01
CILE/ 0.5 M H_2SO_4	Blank	30.96	8.16×10^{6}	28.30	-114.51
	1	33.05	1.10×10^{7}	30.41	-112.03
	2	34.50	1.81×10^{7}	31.86	-107.88
	3	34.73	1.85×10^{7}	32.09	-107.67
	4	35.41	2.28×10^{7}	32.77	-105.97
	5	41.50	1.92×10^{8}	38.86	-88.22
CIRE/ 1 M HCl	1	90.23	2.69×10^{15}	87.59	48.60
	2	91.66	4.15×10^{15}	89.03	52.20
	3	92.62	5.00×10^{15}	89.98	53.73
	4	101.18	1.02×10^{17}	98.54	78.83
	5	101.54	1.04×10^{17}	98.90	78.99
CIRE/ 0.5 M H_2SO_4	1	35.33	2.57×10^{7}	32.69	-104.97
	2	36.45	3.66×10^{7}	33.81	-102.02
	3	37.58	5.34×10^{7}	34.94	-98.89
	4	39.40	9.91×10^{7}	36.76	-93.75
	5	44.87	7.13×10^{8}	42.23	-77.33

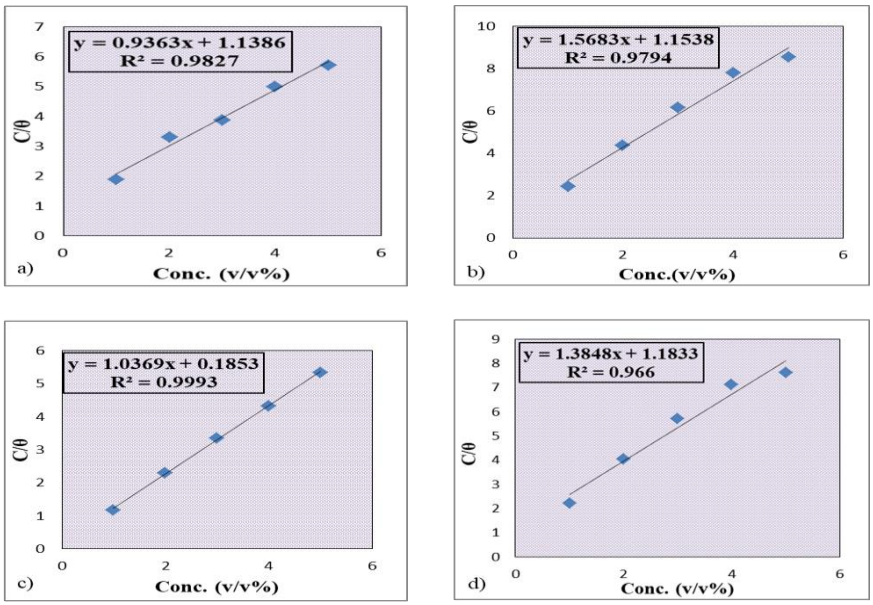

Fig. 7.7: Langmuir adsorption isotherm of CILE and CIRE on mild steel in 1 M HCl (a & c) and 0.5 M H_2SO_4 (b & d)

Table 7.5: Langmuir adsorption parameters of mild steel in 1 M HCl and 0.5 M H_2SO_4 with CILE and CIRE from weight loss measurements at room temperature

Inhibitor	Medium	ΔG^0_{ads} ($kJmol^{-1}$)	K_{ads}	R^2
CILE	1 M HCl	27.01	878.27	0.9827
	0.5 M H_2SO_4	26.97	866.70	0.9794
CIRE	1 M HCl	31.55	5396.6	0.9993
	0.5 M H_2SO_4	26.91	845.09	0.9660

Electrochemical impedance spectroscopy

Kinetics and mechanism of metal dissolution process can be interpreted using electrochemical impedance spectroscopy (EIS). Fig. 7.8 and Fig. 7.9 reveals the Nyquist and Bode plots for mild steel in 1 M HCl and 0.5 M H_2SO_4 with and without extracts of *Clerodendrum infortunatum* at room temperature. These plots have been seen with similar shapes for all concentrations, including blank, which means the mechanism of metal dissolution was almost exact for inhibited and uninhibited metal. A single capacitive loop of the impedance spectra suggested that the charge transfer reactions were predominant reactions involved in metal corrosion. The imperfect semicircular capacitive loop was observed as a consequence of the roughness and inhomogeneity on the metal surface[192].

Moreover, semicircle diameter in the presence of CILE and CIRE was more extensive than that in acid solution in the absence of extracts. On adding the concentration of extracts, the diameter of Nyquist plots magnified, reinforcing the inhibitive film. This result showed that the impedance of mild steel immersed in acid solution with CILE and CIRE increased with the concentration of extracts and caused the maintenance of excellent inhibitive power. The parameters obtained from Nyquist plots and calculated inhibition efficiencies are tabulated in Table 7.6. It has been noticed that as the concentration of CILE and CIRE increased, the double-layer capacitance (C_{dl})

lowered and charge transfer resistance (R_{ct}) enhanced. This lowering of C_{dl} values was related to imperfections on the metal surface. This relation was simulated through a constant phase element. So, capacitance can be derived using equation (51).

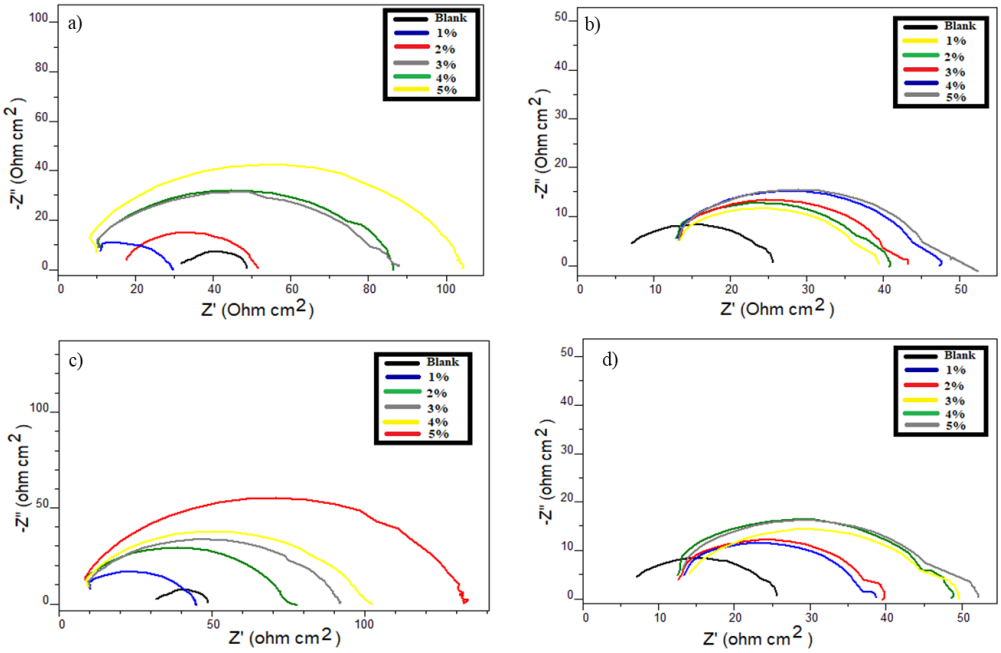

Fig. 7.8: Nyquist plots of mild steel with CILE and CIRE in 1 M HCl (a & c) and in 0.5 M H_2SO_4 (b & d)

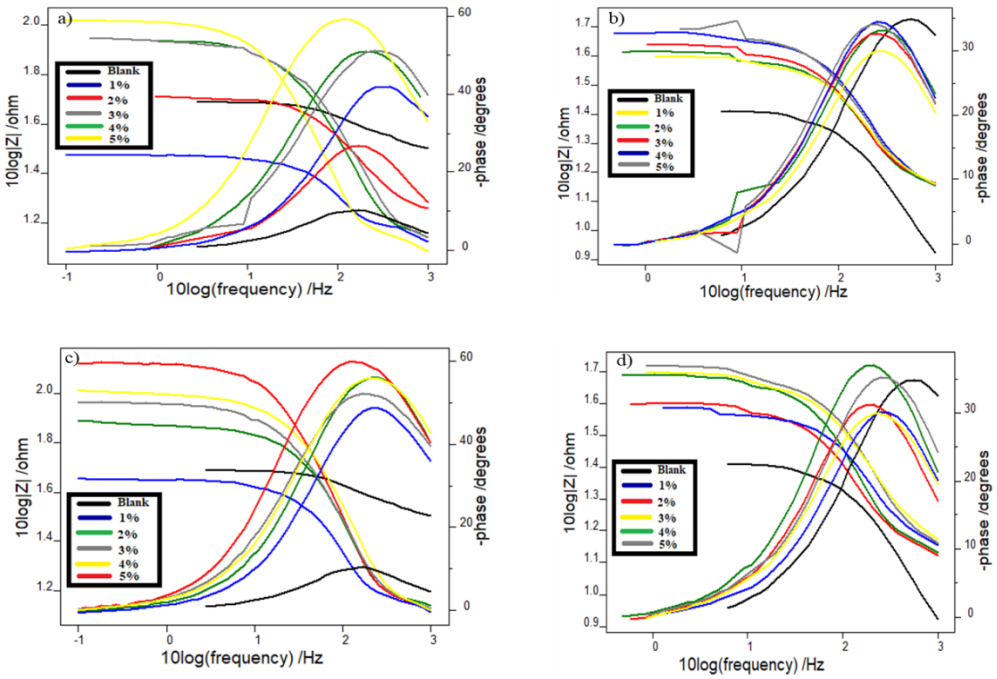

Fig. 7.9: Bode plots of mild steel with CILE and CIRE in 1 M HCl (a & c) and in 0.5 M H_2SO_4 (b & d)

A higher R_{ct} value indicates slower corroding metal. It was worth mentioning that CIRE in HCl solution possessed a higher R_{ct} value among the 4 systems of acid solutions. So, better inhibition efficiency of CIRE in 1 M HCl solution was confirmed by EIS. Bode plots demonstrated that phase angle peaks became larger and broader when the concentration of CILE and CIRE increased[193].

Electrochemical results were simulated to pure electric models by Randle's equivalent circuit (Fig. 1.8). It made possible the calculation of numerical values analogous to all the characteristics of the electrochemical system under study. Inhibition efficiencies of CILE and CIRE calculated from weight loss measurements were in exact reasonably match.

Table 7.6: Impedance parameters of mild steel in 1 M HCl and 0.5 M H_2SO_4 with and without CILE and CIRE

Inhibitor	Conc. (v/v %)	1 M HCl			0.5 M H_2SO_4		
		R_{ct} (Ωcm^2)	C_{dl} (μFcm^{-2})	η_{EIS}%	R_{ct} (Ωcm^2)	C_{dl} (μFcm^{-2})	η_{EIS}%
CILE	Blank	15.7	78.8	-	18.1	47.4	-
	1	30.8	72.8	49.02	28.9	45.2	37.37
	2	31.7	56.5	50.47	33.1	41.0	45.31
	3	70.9	54.7	77.85	33.6	40.5	46.13
	4	71.5	53.4	78.04	35.8	39.4	49.44
	5	92.4	46.2	83.01	36.3	38.8	50.13
CIRE	1	35.8	76.7	56.14	32.7	46.9	44.64
	2	64.6	60.5	75.69	34.1	45.8	46.92
	3	77.6	70.2	79.76	35.3	45.4	48.72
	4	86.8	55.9	81.91	36.5	44.6	50.14
	5	120.0	53.4	86.91	52.8	43.6	65.71

Potentiodynamic polarization studies

Tafel and linear polarization plots for mild steel in 1 M HCl and 0.5 M H_2SO_4 in the absence and presence of CILE and CIRE at room temperature are exhibited in Fig. 7.10 and Fig. 7.11. Potentiodynamic polarization parameters from both Tafel and linear polarization plots are shown in Table 7.7. Fig. 7.10 and Fig. 7.11 delineates that the shape of Tafel and linear polarization plots were the same in acid solutions with and

without extracts. However, extracts to acid solutions increased corrosion current density values (i_{corr}) and decreased corrosion rate irrespective of medium, indicating corrosion inhibition performance of extracts.

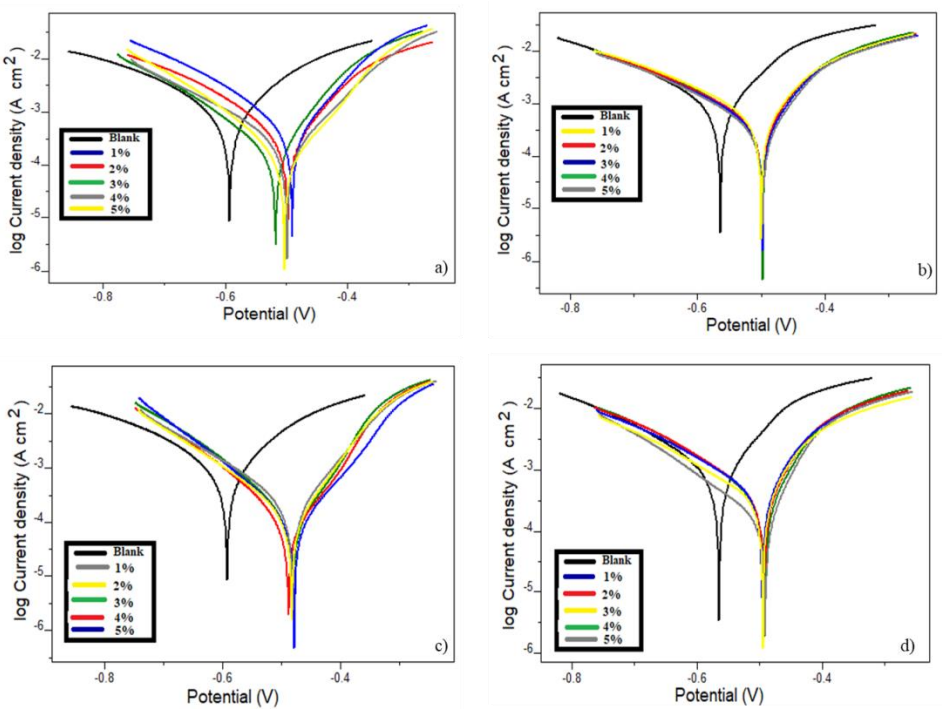

Fig. 7.10: Tafel plots of mild steel with CILE and CIRE in 1 M HCl (a & c) and in 0.5 M H_2SO_4 (b & d)

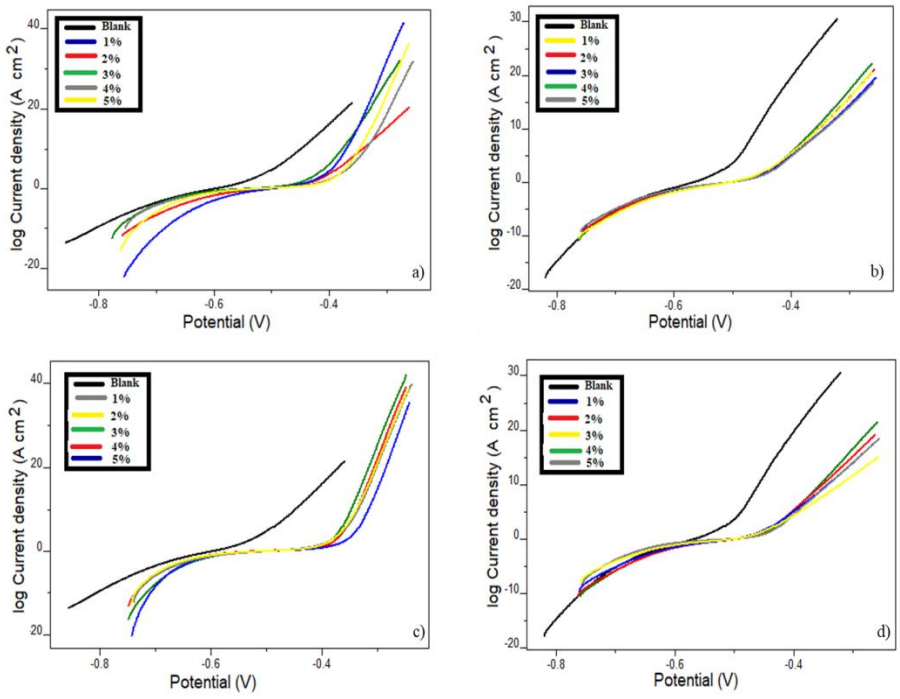

Fig. 7.11: Linear polarization plots of mild steel with CILE and CIRE in 1 M HCl (a & c) and 0.5 M H_2SO_4 (b & d)

It was inferred from Table 7.7 that the corrosion potential (E_{corr}) values of the system with CILE and CIRE shifted to noble values compared to the system without extracts. Both anodic and cathodic slopes were diverted for the sweeps at the various extract concentrations, indicating that CILE and CIRE operate as mixed-type corrosion inhibitors[194]. This result evinced that the components of both extracts in acid media get adsorbed onto both anodic and cathodic sites of the mild steel surface.

According to Tafel data, the increasing order of inhibition efficiency was $CIRE_{HCl}$> $CILE_{HCl}$>$CIRE_{H_2SO_4}$> $CILE_{H_2SO_4}$ and corresponding efficiencies were 92.57%, 87.82%, 66.09% and 51.79% respectively. Again, this result pointed up the potency of CIRE over CILE in inhibiting mild steel against acid attack and agreed with the results acquired from weight loss measurements.

Table 7.7: Potentiodynamic polarization parameters of mild steel in 1 M HCl and 0.5 M H_2SO_4 with and without CILE and CIRE

Inhibitor/ Medium	Tafel data						Polarization data	
	Conc. (v/v %)	$-E_{corr}$ (mV)	i_{corr} (μAcm^2)	b_a (mV/dec)	$-b_c$ (mV/dec)	η_{pol}%	R_p (Ω)	η_{Rp}%
CILE/ 1 M HCl	Blank	597.9	1240	166	221	-	33.14	-
	1	484.6	599.0	97	163	51.69	68.98	51.95
	2	508.9	549.0	132	171	55.72	72.36	54.20
	3	540.5	305.0	110	141	75.40	105.0	68.43
	4	489.7	255.0	96	171	78.80	139.8	76.29
	5	485.9	151.0	77	133	87.82	181.25	81.71
CILE/ 0.5 M H_2SO_4	Blank	602.2	1616	184	193	-	25.30	-
	1	540.6	987.0	188	200	38.92	42.60	40.61
	2	549.5	916.0	191	189	43.31	44.99	43.76
	3	550.8	867.0	195	191	46.34	48.09	47.39
	4	542.9	860.0	174	184	46.78	48.29	47.60
	5	548.5	779.0	185	182	51.79	51.19	50.57
CIRE/ 1 M HCl	1	476.6	220.0	86	156	82.28	109.9	81.57
	2	483.2	154.0	81	139	87.60	203.5	83.71
	3	472.7	150.0	71	129	87.92	223.2	85.15
	4	468.0	99.9	66	130	91.95	289.8	88.56
	5	460.8	92.2	71	121	92.57	211.0	89.34
CIRE/ 0.5 M H_2SO_4	1	552.4	891.0	199	187	44.96	44.96	43.72
	2	547.6	887.0	188	180	45.21	47.02	46.19
	3	543.6	805.0	174	174	50.27	47.05	46.22
	4	561.7	741.0	207	179	54.23	56.30	55.06
	5	572.2	549.0	183	145	66.09	64.11	60.53

According to polarization data, R_p values were augmented in the inhibited solution related to the uninhibited solution suggesting that CILE and CIRE protected mild steel in the acid medium. The trend of inhibition efficiency as a function of the concentration of CILE and CIRE observed for EIS and potentiodynamic polarization measurements matched linear polarization measurements.

Scanning electron microscopy

Fig. 7.12 displays SEM images of polished metal surface, mild steel surface after immersion in 1 M HCl with and without 5 v/v% CILE and CIRE for 24 hours. Fig. 7.12 a) represents SEM image of mild steel surface after polishing. Fig. 7.12 b) evident that the mild steel surface extensively corroded in HCl medium in the absence of extracts. But, in the presence of both extracts, the deterioration was diminished as disclosed in the SEM images (c) and (d), which were comparatively smooth and less damaged than the metal used in the blank experiment. It has also been noted that the mild steel surface with CIRE (d) was more smooth and undamaged than CILE (c). This observation further proved the higher inhibition power of CIRE over CILE.

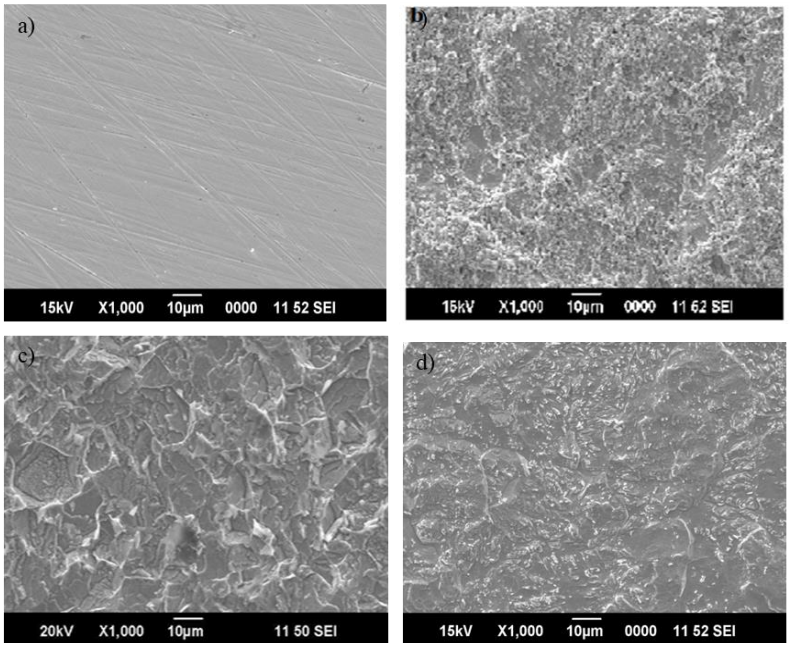

Fig. 7.12: SEM images of the surface of mild steel a) bare b) in 1 M HCl c) in 1 M HCl with CILE d) in 1 M HCl with CIRE

Quantum mechanical calculations

Spatial and electronic structures of an inhibitor have a crucial role in determining its inhibition efficiency. Quantum mechanical parameters such as energies of highest occupied molecular orbital (E_{HOMO}), lowest unoccupied molecular orbitals (E_{LUMO}), energy gap (ΔE), ionization energy (I), electron affinity (A), chemical potential (μ), electronegativity (χ), chemical hardness (η) and the number of electrons transferred (ΔN) of two significant components of *Clerodendrum infortunatum* plant extract 1) Clerodin 2) Scutellarin are given in Table 7.8. The optimized geometry, HOMO and LUMO of Clerodin and scutellarin are shown in Fig. 7.13. If the energy gap between HOMO and LUMO of an inhibitor is small, it will possess inhibition effectiveness since the ionization energy is low. Moreover, a lower ΔE value reflects the high stability of an inhibitor. Table 7.8 shows that the ΔE value of clerodin was lower than scutellarin, indicating a prominent interaction of clerodin molecules with the mild steel surface. This interaction was denoted by electron donation. Thus improved inhibition power of CIRE over CILE revealed the presence of myriads of clerodin molecules in CIRE.

According to FMO theory, E_{HOMO} values of an inhibitor determine whether it can donate its electrons to the metal surface, i.e. higher the E_{HOMO} values increase the ability to donate electrons from inhibitor to vacant metal d-orbital[53]. Or it can be said that lower the E_{LUMO} values favour the acceptance of electrons by the inhibitor molecules. From Table 7.8, it has been noted that E_{HOMO} values are as follows clerodin (-2.176 eV) > scutellarin (-3.12 eV), which recommends that the electron-donating capacity of clerodin was the highest. This was ascribed to the greater extent of adsorption of clerodin molecules over the mild steel surface.

In clerodin, the presence of oxygen moieties is relatively more than scutellarin. It may enhance the electron-donating capacity of clerodin molecules over the other.

Scutellarin has only one -OH moiety. Lower electronegativity (χ) of an inhibitor facilitates the transfer of electrons from the molecules to higher electronegativity possessed metals. During the inhibition reaction between mild steel and extract molecules, electrons move from the extract molecules with lower χ to higher χ until their chemical potentials become equal. If the value of $\Delta N < 3.6$, a molecule incline to donate electrons to the metal surface. So, the inhibition efficiency enhances with respect to electron donation of the inhibitor molecules to the metal surface. The number of electrons transferred from inhibitor molecules follows the order clerodin (1.938) > scutellarin (1.299).

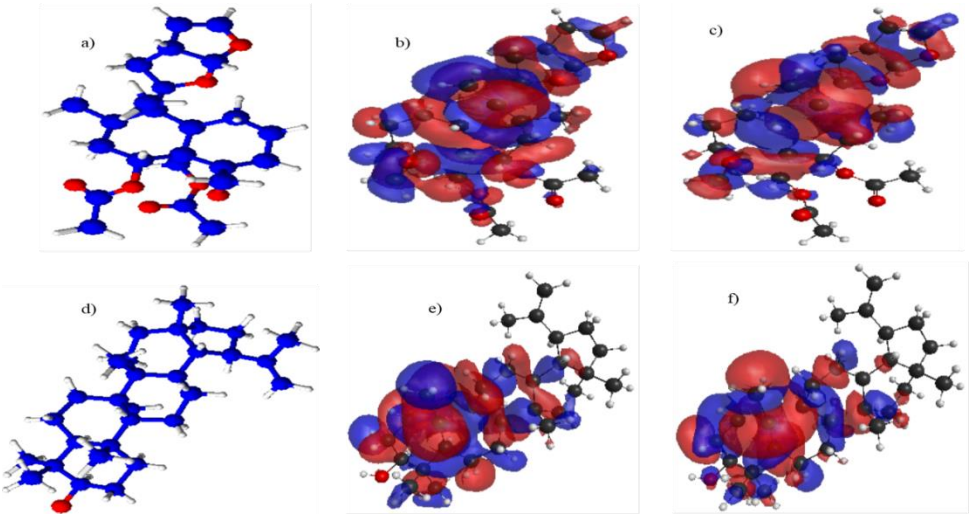

Fig. 7.13: a) Optimized geometry, b) HOMO and c) LUMO of clerodin; d) Optimized geometry, e) HOMO and f) LUMO of scutellarin

Table 7.8: Quantum mechanical parameters (in eV) of clerodin (I) and scutellarin (II)

Molecule	E_{HOMO}	E_{LUMO}	ΔE	I	A	μ	χ	η	ΔN
I	-2.176	1.177	3.35	2.17	-1.17	-0.49	0.49	1.67	1.93
II	-3.120	1.732	4.85	3.12	-1.73	-0.69	0.69	2.42	1.29

Statistical analysis

❖ ***Optimization of factors for inhibition efficiency (IE%)***

Response surface methodology (RSM) provides optimized conditions for tested parameters to acquire a good response. It was evident from weight loss measurements

that the corrosion inhibition efficiency of extracts greatly influenced its concentration and operating temperature, and CIRE showed excellent inhibition performance in 1 M HCl medium over CILE. So, corrosion inhibition efficiency of CIRE and parameters such as temperature and concentration of CIRE in 1 M HCl medium were linked through regression analysis. Two parameters used in the RSM technique are temperature in K (X_1) and concentration of CIRE in v/v% (X_2).

Central composite design (CCD) was employed to study the impact of temperature (X_1) and concentration of CIRE (X_2) on inhibition efficiency (IE%). Table 7.9 shows all the experimental runs in CCD and corresponding predicted inhibition efficiency by optimizing the two parameters.

Table 7.9: Experimental and predicted IE% from the weight loss measurements and CCD

Temp (X_1)	Conc. (X_2)	IE%		Residual
		Experimental	Predicted	
313	5	88.98	89.44	0.46753
333	1	51.48	53.37	1.89273
313	1	75.56	76.44	0.88033
333	5	69.51	70.98	1.47793
313	3	82.25	83.80	1.55793
323	5	78.15	79.18	1.03073
333	3	63.28	63.04	-0.23567
323	1	63.58	63.86	0.28953
323	3	70.69	72.38	1.69913

A full quadratic model was developed to understand the influence of inhibitor efficiency on the independent parameters in selected ranges:

$$IE = 1532 - 7.91X_1 - 13.481X_2 + 0.01037X_1^2 - 0.216X_2^2 + 0.0576X_1X_2 \quad (57)$$

Validity of this quadratic equation can be evaluated from residual plots given in Fig. 7.14. It contains four different plots. On inspection of the normal probability plot, it has been observed that this full quadratic equation for inhibition efficiency was fixed to the normal distribution. It implied that the derived model needs no response

transformation, and there were no noticeable complications with normality. Versus fits plot revealed that there was a constancy in the variance of observations for all responses. Histogram of residuals pointed out that the residuals were allocated uniformly for all frequencies. Versus order plot disclosed that points of observed runs were scattered randomly, maintaining the fixed area of residuals which substantiated the model's precision. In summary, all four plots corroborated the accuracy of the model to demonstrate the influence of parameters on the inhibition efficiency of CIRE.

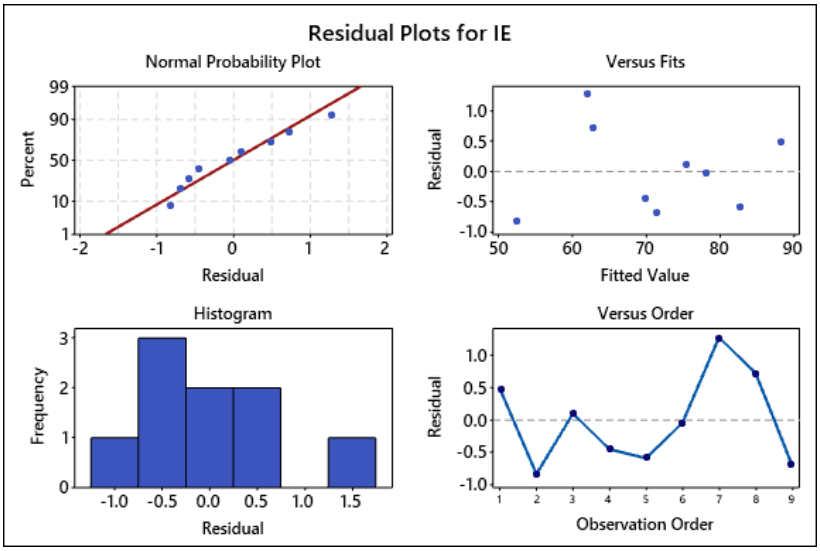

Fig. 7.14: Residual plots for inhibition efficiency

Table 7.10 describes the analysis of variance for corrosion inhibition efficiency. P-value was the superior value in Table 7.10 which establishes the significance of the variable[162]. The adopted value of α, degree of essentialness, was 0.05. On close observation to Table 7.10, it can be said that only for the linear terms the P-value was found to be less than α, which means linear terms significantly affect the response. There was little effect on IE for square and two-way interaction terms. Pareto chart (Fig. 7.15) interprets that only linear terms predominantly influenced the inhibition efficiency. Among the two linear parameters, the temperature was a more significant term than concentration. It was found that squared terms X_1^2, X_2^2 and two–way interaction term

X_1X_2 possess no considerable effect on the inhibition efficiency. Value of coefficient (R^2) obtained for the predicted model was 0.9891, which inferred the best fit quadratic model for the experimental results. Therefore, the outcomes can be easily analyzed by the model.

Table 7.10: Analysis of variance for corrosion inhibition efficiency

Source	DF	Adj SS	Adj MS	F-Value	P-Value
Model	5	1013.38	202.677	146.67	0.001
Linear	2	1004.43	502.216	363.44	0.000
Temp	1	651.46	651.458	471.45	0.000
Conc	1	352.97	352.973	255.44	0.001
Square	2	3.64	1.820	1.32	0.389
Temp *Temp	1	2.15	2.149	1.56	0.301
Conc *Conc	1	1.49	1.491	1.08	0.375
2-Way Interaction	1	5.31	5.313	3.84	0.145
Temp *Conc	1	5.31	5.313	3.84	0.145
Error	3	4.15	1.382		
Total	8	1017.53			

DF: degrees of freedom, Adj SS: adjusted sum of squares, Adj MS: adjusted mean of squares, F: Fischer's F-test value, P: probability

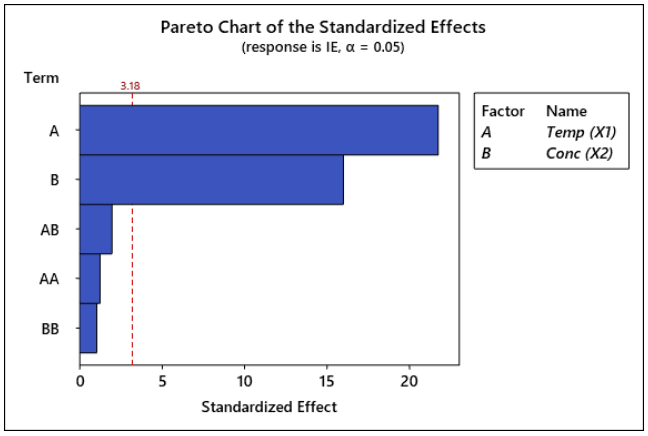

Fig. 7.15: Pareto chart of the standardized effects of mild steel

The influence of two parameters studied independently on IE% and is shown in the Main effects plots (Fig. 7.16). It was observed that temperature is inversely proportional to IE% while CIRE concentration is directly proportional to IE%. It can be inferred that CIRE molecules are adsorbed on the metal surface through physisorption mode. So, IE% decreased with higher temperatures. As the concentration of CIRE

increased, the coverage of active sites on the metal surface increased. Similar observations were found with weight loss measurements.

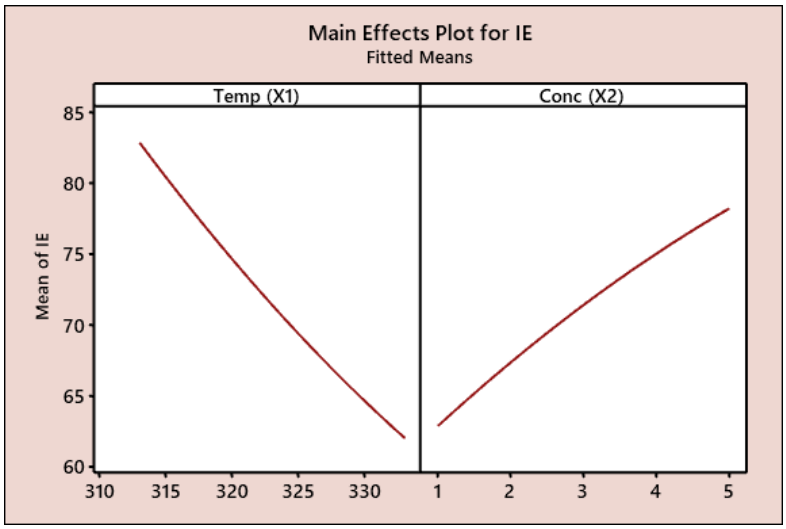

Fig. 7.16: Main effects plots for inhibition efficiency of mild steel in 1 M HCl

Interrelation of the parameters on IE% was measured using a contour and 3-D surface plot vs two independent parameters[195] in Fig. 7.17 a) and Fig. 7.17 b), respectively. It has been evident from Fig. 7.17 that the highest IE% was achieved for 5 v/v% concentration of CIRE at 313 K operating temperature. It can be said that higher temperature leads to an increase in the corrosion rate and, thus, decreased IE%.

❖ ***Response Optimization***

The CIRE concentration and temperature at which maximum IE% were acquired using the desirability function method of response optimization technique. Herein, independent parameters were optimized to maximum, and the corresponding plot is presented in Fig. 7.18. The optimum conditions of temperature and concentration were 313 K and 5 v/v %, which corresponds to 88.4931% inhibition efficiency, i.e. the best outcome for the response.

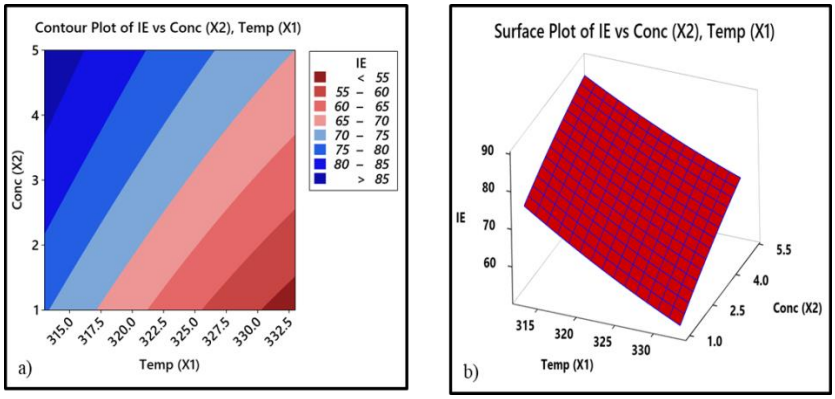

Fig. 7.17: a) Contour and b) 3-D surface plot for corrosion inhibition efficiency

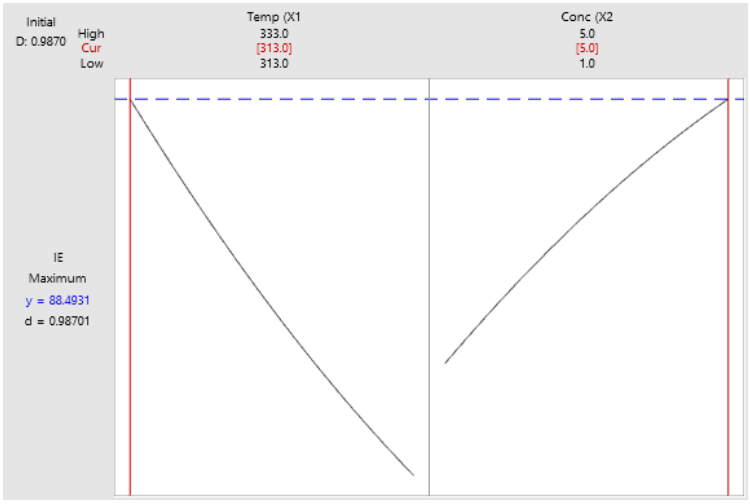

Fig. 7.18: Response optimization plot for inhibition efficiency

Conclusions

- The corrosion inhibition behaviour of *Clerodendrum infortunatum* leaf and root extracts on mild steel in 1 M HCl and 0.5 M H_2SO_4 were investigated using experimental and quantum mechanical techniques.
- Electrochemical studies disclosed that CIRE and CILE possessed fairly good inhibition efficiencies.
- The inhibition efficiencies calculated from EIS and polarization parameters were in exact agreement.
- The adsorption of CILE and CIRE on mild steel in both acid media was according to Langmuir adsorption isotherm.

- The quantum mechanical calculations for the main phytochemicals clerodin and scutellarin evidently supports the experimental results.
- The SEM images showed the protective power of the extracts on the mild steel surface.
- Predicted inhibition efficiency of CIRE at different CIRE concentrations and operating temperature in 1 M HCl evaluated by RSM was in perfect agreement with the data obtained from weight loss measurements.